Appl. Sci. **2015**, *5*, 532-543; doi:10.3390/app5030532

OPEN ACCESS

applied sciences

ISSN 2076-3417

www.mdpi.com/journal/applsci

Article

Microwave-Assisted Conversion of Levulinic Acid to γ-Valerolactone Using Low-Loaded Supported Iron Oxide Nanoparticles on Porous Silicates

Alfonso Yepez, Sudipta De, Maria Salud Climent, Antonio A. Romero and Rafael Luque *

Departamento de Química Orgánica, Universidad de Córdoba, Campus de Rabanales, Edificio Marie Curie (C-3), Ctra Nnal IV-A, Km 396, E14014, Cordoba, Spain; E-Mails: z22yegaa@uco.es (A.Y.); qo2susus@uco.es (S.D.); qo1clbem@uco.es (M.S.C.); qo1rorea@uco.es (A.A.R.)

* Author to whom correspondence should be addressed; E-Mail: q62alsor@uco.es; Tel.: +34-95721050; Fax: +34-957212066.

Academic Editor: Rajender S. Varma

Received: 6 July 2015 / Accepted: 31 August 2015 / Published: 9 September 2015

Abstract: The microwave-assisted conversion of levulinic acid (LA) has been studied using low-loaded supported Fe-based catalysts on porous silicates. A very simple, productive, and highly reproducible continuous flow method has been used for the homogeneous deposition of metal oxide nanoparticles on the silicate supports. Formic acid was used as a hydrogen donating agent for the hydrogenation of LA to effectively replace high pressure H_2 mostly reported for LA conversion. Moderate LA conversion was achieved in the case of non-noble metal-based iron oxide catalysts, with a significant potential for further improvements to compete with noble metal-based catalysts.

Keywords: flow nanocatalysis; conversion of levulinic acid; hydrogenation; GVL; supported nanoparticles

1. Introduction

γ-Valerolactone (GVL) has been recently considered as a new renewable liquid for gasoline and diesel fuel oxygenate due to its comparable fuel characteristics to those of fossil-based fuels [1]. Some drawbacks, including high water solubility and smaller cetane number as compared with diesel fuels limit actual applications of GVL in the transportation sector. However, these weaknesses can be

overcome by upgrading GVL into useful liquid hydrocarbon fuels through various catalytic cascade processes [2,3]. GVL can consequently serve as a high-valued intermediate or platform chemical for the production of biofuels. Apart from the excellent fuel properties, GVL is also regarded as a promising sustainable liquid from biomass for the production of other carbon-based chemicals because of its renewable nature, non-toxicity, stability, and biodegradability [4]. Since GVL has the ability to solubilize all products from cellulose deconstruction, it can be used as a biphasic solvent system in biorefineries [5,6]. GVL has also recently shown very good effectiveness in thermocatalytic production of soluble sugars from corn stover and wood at high yields [7]. Complete solubilization of biomass, including lignin fractions, could be achieved in a dilute aqueous phase-GVL medium to promote a thermocatalytic saccharification of biomass into monosaccharides.

Many reports are available on the catalytic conversion of LA to GVL. While different homogeneous catalysts such as Ru-complexes, including Shvo catalyst [8–10], iridium pincer complexes [11,12] were used with excellent performance even under mild reaction conditions, they are arguably not suited to targeted GVL production as the high boiling point of GVL (207–208 °C) makes product/catalyst separation uneconomical by means of distillation. In this regard, several heterogeneous catalytic systems have been reported in the last few years with noble metals including Ru [13–15], Pd [16,17], Pt [18], and Au [19] as active metal species generating high yields of GVL from LA. An excellent approach of LA hydrogenation was studied under supercritical CO_2 over Ru/Al_2O_3 and Ru/SiO_2 catalysts that produced 99% GVL (200 °C and 20 MPa H_2) [20]. There are also some reports on bimetallic catalysts such as Ru-Sn/C [21], RuNi-OMC [22], *etc.*, which showed improved selectivity at high GVL yields. However, the activity and stability of many noble metal catalysts, especially Ru and Pt catalysts, is not ideal due to catalyst deactivation and substantial active metal leaching [13,23,24]. In addition, the use of noble metals for GVL production is not suitable for commercial applications and attention should be consequently paid to the development of non-noble metal systems with high activity and selectivity to GVL production.

Hengne and Rode reported copper-based catalysts over ZrO_2 and Al_2O_3 for the hydrogenation of LA and its methyl ester, resulting in quantitative conversion with >90% GVL selectivity [25]. In another report, a series of base-metal (Ni, Co, Cu, and Fe) and metal oxides (Mo, V, and W oxides) co-loaded carbon were tested for the hydrogenation of LA [26]. Ni-MoO_x/C showed the highest activity with 97% GVL yield which was probably due to the co-presence of metallic Ni^0 species and partially reduced MoO_2. Aqueous phase hydrogenation of LA using Mo_2C catalysts provided 99% LA conversion with 90% GVL selectivity at 30 bar H_2 and 200 °C [27]. The catalytic transfer hydrogenation (CTH) of ethyl levulinate (EL) in isopropanol was also reported using a porous Zr-containing catalyst (Zr-HBA) with a phenate group that produced 94.4% GVL [28]. The presence of the phenate group increased the basicity of the catalyst, which significantly favored the CTH process. Another Zr-based catalyst (Zr-Beta zeolite) was also studied for the Meerwein-Ponndorf-Verley (MPV) reduction of LA in different secondary alcohols in both batch and continuous flow reactors [29]. This catalyst also showed excellent activity with >99% GVL yield.

In our aim to develop advanced catalytic nanomaterials for biomass valorization processes, herein we report a highly-reproducible continuous flow method for the preparation of supported iron oxide catalysts on porous silicates and their application in the microwave-assisted conversion of LA to GVL. Inspired by our previous report in the hydrogenation of LA that employed formic acid (FA) as a

hydrogen-donating solvent [30], we have applied here the same state-of-the-art in the presence of low loaded iron-based catalysts (typically 0.5 wt%). Previous findings related to this work have also proved the efficiency of FA as both solvent and hydrogen donating agent in LA hydrogenation [31,32].

2. Experimental Section

2.1. Materials Synthesis

2.1.1. Synthesis of Al- and Zr-SBA-15

Al-SBA-15 materials (Si/Al = 20 ratio) were synthesized according to a previously reported protocol [33]. A solution (300 mL) of hydrochloric acid at pH = 1.5 was prepared, then 8.07 g of the surfactant (poly (ethylene-glycol)-block (P123 Aldrich) was added to this solution. The mixture was stirred until a final transparent solution was obtained. 0.82 g of aluminum isopropoxide (98 wt%, Aldrich, St Louis, MO, USA) was then added to the mixture followed by 18 mL TEOS (tetraethylortosilicate) dropwise (time 5–10 min). The final gel was stirred for 24 h and introduced into a furnace at 100 °C, t = 24 h. The products obtained were filtered and calcined at 600 °C for 8 h (2 h in a nitrogen atmosphere and 6 h in air). A Zr containing analogous silicate was synthesized adding the needed quantity of Zr (0.942 g Zr (IV) oxonitrate hydrate) to the synthesis gel to achieve a theoretical Si/(Zr) ratio of 20 in the final material, ZrSBA-15.

2.1.2. Continuous Flow Synthesis of Supported Iron Oxide Nanoparticles on Al- and Zr-SBA-15

The continuous flow deposition of iron oxide nanoparticles on Al-SBA-15 was performed under a series of conditions using a recently reported, innovative, continuous flow setup depicted in Figure 1 [33]. A stainless-steel reactor (1.2 cm^3 volume) was packed with Al-SBA-15 support (typically 0.5 g), set between two plugs of quartz wool to prevent the solid support to move in the reactor upon pumping in the flow of the solution of the metal precursor. Separately, a 0.5 wt% Fe solution in ethanol was prepared using $FeCl_2 \cdot 4H_2O$ (0.89 g in 50 mL ethanol) as the Fe precursor. The solution was filtered off prior to flowing it through the system to avoid the presence of any undissolved metal precursor. The system started with pumping a solution of pure ethanol (0.5 $mL \cdot min^{-1}$, 5 min) through the catalyst bed to wet the catalyst. The temperature of the reactor was then set to 100 °C and the system was changed to the 0.5 wt% Fe solution which was pumped through the system at different flow rates. The incorporation was conducted under optimized flow rates (0.5 $mL \cdot min^{-1}$) and residence time conditions (8 min). At the end of the continuous flow process, the system was again switched to ethanol which was pumped through the Fe-incorporated catalyst at 100 °C in order to remove physisorbed/unreacted Fe species on the catalyst. Materials were then recovered from the reactor, ground with a pestle and a mortar and subsequently oven-dried at 100 °C. Final materials were calcined at 400 °C for 4 h under air. For simplicity, Fe/Al-SBA 0.5 $mL \cdot min^{-1}$ materials are denoted as (Fe-AlCF), where this material was prepared with a 0.5 wt% theoretical loading of Fe at a flow rate of 0.5 mL min^{-1} during 8 min of reaction incorporation at 100 °C. Similarly, Fe/Zr-SBA 0.5 $mL \cdot min^{-1}$ (Fe-ZrCF) stands for a material prepared with a 0.5 wt% theoretical loading of Fe at a flow rate of 0.5 $mL \cdot min^{-1}$ during 8 min of reaction incorporation at 100 °C. Samples were highly reproducible from batch to batch.

Figure 1. Experimental setup for the continuous flow preparation of Fe/Al(Zr)-SBA-15 materials.

Similarly, a Pd-containing Al-SBA-15 material (PdAlCF) was also synthesized under identical deposition conditions to achieve a loading around 0.5 wt% Pd in the final material.

2.1.3. Mechanochemical Synthesis of Pd/Al-SBA-15

A Pd/Al-SBA-15 material was also synthesized for comparative purposes following a previously reported mechanochemical protocol [34,35]. Needed quantities of a solid Pd precursor (palladium(II) acetate) to reach theoretical Pd contents of 0.5 wt% Pd (0.021 g palladium acetate) in the materials were milled together with the pre-formed Al-SBA-15 in the solid phase in a Retsch PM 100 planetary ball mill (optimum conditions: 350 rpm, 10 min milling) [34,35]. Upon milling, the final mechanochemical material obtained (denoted as PdAlSBA-BM) was calcined at 400 °C in air for 4 h. A commercial 5% Pd/C catalyst (Sigma-Aldrich) has been also employed as a reference catalyst for comparative purposes.

2.2. Materials Characterization

Materials were characterized using nitrogen physisorption, powder X-Ray diffraction (XRD, PanAnalytic/Philips, Lelyweg, Almelo, The Netherlands), Transmission Electron Microscopy (TEM, JEOL, Peabody, MA, USA) and ICP/MS (Philips, Lelyweg, Almelo, The Netherlands).

Nitrogen adsorption measurements were carried out at 77 K using an ASAP 2000 volumetric adsorption analyzer from Micromeritics (Micromeritics, Norcross, GA, USA). The samples were outgassed for 24 h at 100 °C under vacuum ($P_0 = 10^{-2}$ Pa) and subsequently analyzed. The linear part of the BET equation (relative pressure between 0.05 and 0.30) was used for the determination of the specific surface area. Mean pore size diameter (DBJH) and pore volumes (VBJH) were obtained from porosimetry data.

XRD experiments were recorded on a PanAnalytic/Philips X'pert MRD diffractometer (PanAnalytic/Philips, Lelyweg, Almelo, The Netherlands) (40 kV, 30 mA) using Cu Kα ($\lambda = 0.15418$ nm) radiation. Scans were performed over a 2θ range from 10 to 80, at step size of 0.018° with a counting

time per step of 5 s. Transmission electron microscopy (TEM) images of the samples were obtained on a JEM 2010F (JEOL, Peabody, MA, USA) microscope and Phillips Analytical FEI Tecnai 30 microscope (FEI Tecnai, Hillsboro, OR, USA).

XPS measurements were performed in an ultra high vacuum (UHV) multipurpose surface analysis system (Specst model, Berlin, Germany) operating at pressures $<10^{-10}$ mbar using a conventional X-ray source (XR-50, Specs, Mg-Ka, 1253.6 eV) in a "stopand-go" mode to reduce potential damage due to simple irradiation. The survey and detailed Fe and Cu high-resolution spectra (pass energy 25 and 10 eV, step size 1 and 0.1 eV, respectively) were recorded at room temperature using a Phoibos 150-MCD energy analyser (Phoibos, Berlin, Germany). Powdered samples were deposited on a sample holder using double-sided adhesive tape and subsequently evacuated under vacuum ($<10^{-6}$ Torr) overnight. Eventually, the sample holder containing the degassed sample was transferred to the analysis chamber for XPS studies. Binding energies were referenced to the C1s line at 284.6 eV from adventitious carbon. Deconvolution curves for the XPS spectra were obtained using software supplied by the spectrometer manufacturer.

The metal content in samples was quantified via Inductively Coupled Plasma (ICP) using a Philips PU 70000 sequential spectrometer containing an Echelle monochromator (0.0075 nm resolution) and then coupled to mass spectrometry. Samples were dissolved in a mixture HF-HNO_3-H_2SO_4 and subsequently quantified using ICP/MS at the SCAI of Universidad de Cordoba.

2.3. Catalytic Experiments

Microwave-assisted Conversion of Levulinic Acid to γ-valerolactone

Microwave-assisted reactions were conducted on a pressure-controlled CEM-Discover microwave reactor for a period of time (typically 30 min) at 150 °C under continuous stirring. Samples were then withdrawn from the reaction mixture and analyzed by GC and GC/MS using an Agilent 6890N (Agilent Technologies, Los Angeles, CA, USA) fitted with a SUPELCO EQUITY TM-1 fused silica capillary column (60 m × 0.25 mm × 0.25 μm) and a flame ionisation detector (FID).

In a typical reaction, 0.1 mL levulinic acid, 0.3 mL formic acid and 0.05 g catalyst were added to a Pyrex® vial and microwaved in a pressure-controlled CEM-Discover microwave reactor for 30 min at 300 W maximum power output (within a temperature range of 180–200 °C and a maximum pressure of 250 PSI) under continuous stirring. Samples were then withdrawn from the reaction mixture and analyzed by GC using the previously described method. Products were identified and confirmed by GC-MS as well as ^{1}H and ^{13}C NMR. Response factors of products were obtained from GC analysis employing standard compounds using calibration curves.

Microwave experiments were conducted under closed-vessel mode, generally temperature controlled (by an infra-red probe), where the samples were irradiated with the required power output (settings at maximum power, 300 W) to achieve the desired temperature.

3. Results and Discussion

Inspired by our previous work on the hydrogenation of LA using Cu-containing silica materials, we designed a supported iron oxide catalyst on porous silicates based on our previous report [30,33]. We applied a simple, innovative, and efficient continuous flow methodology for the deposition of iron oxide nanoparticles on porous materials. Textural properties of synthesized materials in this work are summarized in Table 1. All final materials exhibited high surface areas (>600 m^2g^{-1}), in good agreement with typical characteristics of mesoporous SBA-15 materials. The incorporation of Fe in the systems did not have any significant effect on the textural properties of supported materials in terms of surface area, pore size and volume, in good agreement with previously observed surface deposition of Fe species under continuous flow preparation [33]. Fe loading was found to be less than 1 wt%, with a slightly higher loading observed for FeAlCF with respect to FeZrCF. No significant differences were obtained between ICP and EDX analysis, which correlated well with previous synthesized catalytic nanomaterials under flow conditions [33]. Both Pd systems (PdAlCF and PdAlSBA-BM) contained *ca.* 0.5–0.6 wt% Pd as measured by ICP/MS (results not shown), an almost comparable metal loading to that of analogous Fe-containing aluminosilicates from this work regardless of the synthesis protocol.

Table 1. Textural properties and ICP-MS analysis of mesoporous silicates synthesized in this work.

Material	Surface area [a] (m^2g^{-1})	Pore size (nm)	Pore volume [b] (mLg^{-1})	Elemental composition [c] (%)		
				Fe [d]	Al	Zr
Al-SBA-15	720	8.5	0.80	-	2.0	-
Zr-SBA-15	765	7.4	0.74	-	-	4.0
FeAlCF	659	8.2	0.77	0.85 (0.6)	1.1	-
FeZrCF	687	7.0	0.66	0.53 (0.7)	-	3.9
PdAlCF	633	7.9	0.70	-	1.2	-
PdAlSBA-BM	507	8.5	0.92	-	1.1	-
5%Pd/C	1220	<2	1.50	-	-	-

[a] BET surface area was estimated by using a multipoint BET method with adsorption data in the relative pressure range of 0.05–0.30; [b] Mesopore volume was calculated from the isotherm data by using the DFT method, otherwise pore volume was calculated from the isotherm data at a relative pressure of 0.95; [c] Based on ICP-MS and EDX analyses; [d] EDX values in parentheses as an average of three measurements.

Similarly to previously reported work [33], Fe species in the materials were found to correlate to a hematite Fe_2O_3 phase with nanoparticle sizes in the 5–7 nm range (clearly visualizable in the TEM micrographs around the edges, Figure 2).

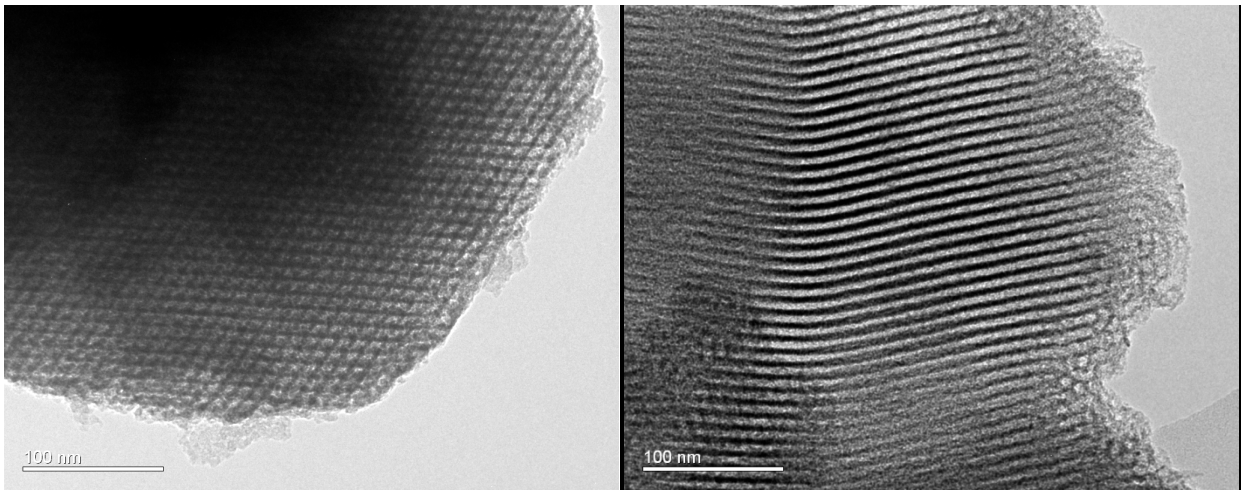

Figure 2. TEM micrographs of FeAlCF (**left**) and FeZrCF (**right**).

Catalytic activities of the investigated catalysts in the hydrogenation of LA have been summarized in Table 2. Reactions were carried out under microwave irradiation (MI) for a quick screening and optimization of reaction conditions. FA served as both solvent and hydrogenating agent which efficiently decomposed under microwave mild heating to provide the needed *in situ* generated hydrogen for the hydrogenation reaction based on previous work by the group on FA-assisted lignin depolymerization [34,35].

Table 2. Liquid-phase microwave-assisted hydrogenation of LA using different catalysts [a].

Entry	Catalyst	Mass catalyst (g)	Conv. (mol%)	TOF (h^{-1})	Selectivity (mol%)			
					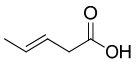	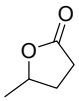	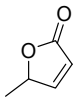	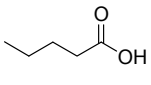
1	Blank	-	<5	-	-	-	-	-
2	Al-SBA-15	0.1	<5	-	-	-	-	-
3	Zr-SBA-15	0.1	<5	-	-	-	-	-
4	FeZrCF	0.05	30	125	22	78	-	-
5	FeAlCF	0.05	20	52	36	64	-	-
6	PdAlCF	0.05	<10	-	-	96	-	4
7	PdAlSBA-BM	0.05	<10	-	-	94	-	6
8	5%Pd/C	0.05	22	19	-	66	27	7
9	5%Pd/C [b]	0.1	33	14	-	88	6	6
10	5%Pd/C	0.1	36	14	-	86	7	7

[a] Reaction conditions: 0.1 mL LA, 0.3 mL FA, 30 min microwave irradiation, 200 °C, 300 W (maximum power output); [b] Reaction run at 150 °C.

The present reaction conditions provided very low LA conversion (<5%) in the absence of catalyst (blank run) and in the presence of the parent Al- and Zr-SBA-15 supports even at 200 °C (Table 2). Gratifyingly, the incorporation of Fe_2O_3 nanoparticles even at low loading (<1 wt%) in newly explored iron-based catalysts provided moderate LA conversion under the investigated reaction conditions (Table 2, entries 4 and 5). Typical LA conversions in the systems were ca. 30% with a *ca.* 45% increase pushing reaction conditions (200 °C, 60 min, 100 mg FeZrCF catalyst). TON values obtained for most active catalysts FeZrCF (62) and FeAlCF (26) and particularly TOF values (Table 2) pointed to a

relatively good activity of the systems per active site as compared to noble metal-based literature reported catalysts [17,19,22,31,32]. GVL selectivity significantly varied from FeAl to FeZr systems (60%–75%), with a maximum of 75%–80%. The combined analysis of GC-MS and NMR also confirmed that significant amounts of interesting C_5 products (e.g., pentenoic acid) were also formed together with major product GVL obtained in the reaction. This was particularly interesting and unexpected in the case of FeAlSBA (Table 2, Scheme 1) for which selectivities of *ca.* 35%–40% to pentenoic acid were observed under the investigated reaction conditions. Comparatively, similarly-prepared flow PdAlCF catalyst and the analogous mechanochemically-prepared Pd nanocatalyst exhibited an almost negligible conversion in the system. These results confirmed that the potential of the proposed Fe-based systems over noble metals under the investigated conditions.

Furthermore, the use of a commercial 5% Pd/C catalyst (*ca.* 10 times higher metal loading) provided only a slightly improved conversion of LA pushing reaction conditions but remarkably reduced TOF values (Table 2). Under comparable conditions (Table 2, entries 4 *vs.* 8) product yields were also inferior for 5% Pd/C as compared to FeZrCF, with also reduced GVL selectivities. Doubling the amount of catalyst, both conversion and GVL selectivity increased up to comparable levels to those observed for FeZrCF, although with significantly different TOF and TON values.

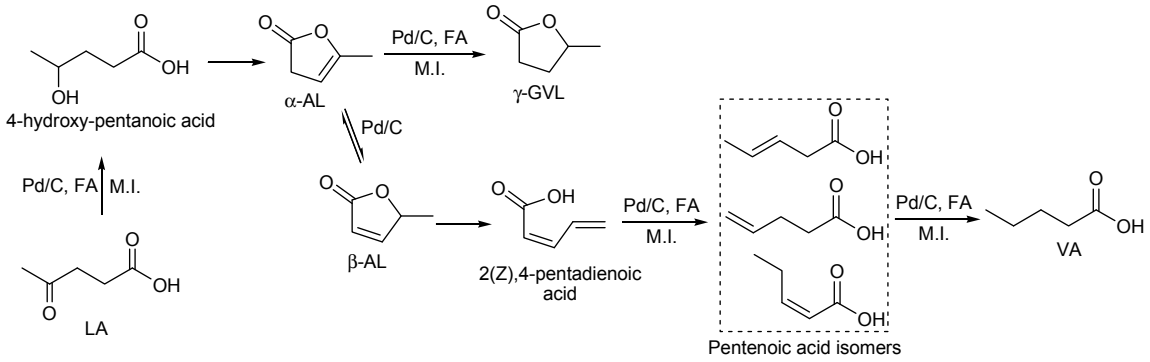

Scheme 1. Reaction pathway for the microwave-assisted hydrogenation of LA in presence of FA using Pd/C catalyst.

Importantly, the catalytic systems based on Fe were found to be stable under the investigated conditions, particularly in the presence of aqueous media and formic acid, exhibiting similar catalytic activities after three uses (only 20% reduction of the initial activity was observed under the microwave-assisted conditions). These results are in good agreement with the good stability of analogous Cu-based systems employed in the conversion of LA under microwave irradiation [30]. Comparative reactions under conventional heating provided no significant activity in the conversion of LA for any of the present catalytic systems even after 12 h of reaction.

GC-MS and NMR analyses of the reaction mixtures revealed that β-angelica lactone (β-AL) and valeric acid (VA) were also formed along with GVL, which points to hydrogenation, isomerization, and ring opening reactions also taking place during LA conversion under the investigated conditions. Interestingly, the higher hydrogen concentration on Pd surfaces led to some extent of the over-hydrogenation product (VA) in each case. These results are in good agreement to those previously reported by the Palkovits group where Ru/C was used for the hydrogenation of α-AL in the presence of external H_2 pressure. According to their observation, this was the first report where VA was obtained as

the product of the α-AL hydrogenation reaction. Similar results were also previously reported for Pd-containing catalysts [3,30].

VA can be obtained from GVL via acid-catalyzed ring-opening reactions [3,23,36,37]. In the present work, we did not observe any VA in case of Fe-based catalysts which indicates that GVL does not undergo ring-opening under the investigated reaction conditions using Fe-based catalysts. In contrast, Pd/C catalysts promote the isomerization of α-AL to β-AL that subsequently undergoes ring-opening to form 2(Z),4-pentadienoic acid (detected in trace quantities in Pd/C reactions) which is further hydrogenated to VA (Scheme 1). Lower catalyst (Pd/C) loading results in reduced GVL selectivities and lower β-AL conversion (Table 2, entry 8). On the other hand, higher catalyst loadings favored the fast kinetics of α-AL hydrogenation (as compared to the α-AL ↔ β-AL isomerization) to give relatively higher GVL selectivity (Table 2, entries 8 *vs.* 9 and 10).

4. Conclusions

In conclusion, supported iron oxide nanocatalysts were synthesized under continuous flow conditions and investigated as efficient catalysts in the microwave-assisted conversion of LA in the presence of formic acid. Activities of these catalysts were compared with noble metal catalysts, resulting in Fe based catalysts providing good LA conversions and GVL selectivities as compared to Pd-based catalyst under otherwise identical conditions. These findings are envisaged to provide an interesting starting point towards the design of alternative non-noble metal catalysts for the conversion of platform chemicals into valuable products.

Acknowledgments

Sudipta De gratefully acknowledges the University Grants Commission (UGC), India and University of Delhi for financial support and necessary journal access during the preparation of this work. Rafael Luque gratefully acknowledges Consejeria de Ciencia e Innovacion, Junta de Andalucia for funding under project P10-FQM-6711 and MICINN for funding under project CTQ2011 28954-C02-02.

Author Contributions

A. Yepez was responsible for catalyst synthesis and design and catalytic work; M.S Climent and A.A. Romero provided the project concept, supervised the work and lead the discussions while S. De and R. Luque were in charge of writing, completing and revising the manuscript from submission to acceptance.

Conflicts of Interest

The authors declare no conflict of interest.

References

1. Bereczky, A.; Lukács, K.; Farkas, M.; Dóbé, S. Effect of γ-valerolactone blending on engine performance, combustion characteristics and exhaust emissions in a diesel engine. *Nat. Resour.* **2014**, *5*, 177–191.
2. Bond, J.Q.; Alonso, D.M.; Wang, D.; West, R.M.; Dumesic, J.A. Integrated catalytic conversion of γ-valerolactone to liquid alkenes for transportation fuels. *Science* **2010**, *327*, 1110–1114.
3. Alonso, D.M.; Bond, J.Q.; Serrano-Ruiz, J.C.; Dumesic, J.A. Production of liquid hydrocarbon transportation fuels by oligomerization of biomass-derived C_9 alkenes. *Green Chem.* **2010**, *12*, 992–999.
4. Horváth, I.T.; Mehdi, H.; Fábos, V.; Boda, L.; Mika, L.T. γ-Valerolactone—A sustainable liquid for energy and carbon-based chemicals. *Green Chem.* **2008**, *10*, 238–242.
5. Wettstein, S.G.; Alonso, D.M.; Chong, Y.; Dumesic, J.A. Production of levulinic acid and gamma-valerolactone (GVL) from cellulose using GVL as a solvent in biphasic systems. *Energy Environ. Sci.* **2012**, *5*, 8199–8203.
6. Qi, L.; Mui, Y.F.; Lo, S.W.; Lui, M.Y.; Akien, G.R.; Horváth, I.T. Catalytic conversion of fructose, glucose, and sucrose to 5-(hydroxymethyl) furfural and levulinic and formic acids in γ-valerolactone as a green solvent. *ACS Catal.* **2014**, *4*, 1470–1477.
7. Luterbacher, J.S.; Rand, J.M.; Alonso, D.M.; Han, J.; Youngquist, J.T. Maravelias, C.T.; Pfleger, B.F.; Dumesic, J.A. Nonenzymatic sugar production from biomass using biomass-derived γ-valerolactone. *Science* **2014**, *343*, 277–280.
8. Chalid, M.; Broekhius, A.A.; Heeres, H.J. Experimental and kinetic modeling studies on the biphasic hydrogenation of levulinic acid to γ-valerolactone using a homogeneous water-soluble Ru-(TPPTS) catalyst. *J. Mol. Catal. A* **2011**, *341*, 14–21.
9. Tukacs, J.M.; Kiraly, D.; Stradi, A.; Novodarszki, G.; Eke, Z.; Dibo, G.; Kegl, T.; Mika, L.T. Efficient catalytic hydrogenation of levulinic acid: A key step in biomass conversion. *Green Chem.* **2012**, *14*, 2057–2065.
10. Fábos, V.; Mika, L.T.; Horváth, I.T. Selective conversion of levulinic and formic acids to γ-valerolactone with the shvo catalyst. *Organometallics* **2014**, *33*, 181–187.
11. Li, W.; Xie, J.H.; Lin, H.; Zhou, Q.L. Highly efficient hydrogenation of biomass-derived levulinic acid to γ-valerolactone catalyzed by iridium pincer complexes. *Green Chem.* **2012**, *14*, 2388–2390.
12. Deng, J.; Wang, Y.; Pan, T.; Xu, Q.; Guo, Q.X.; Fu, Y. Conversion of carbohydrate biomass to γ-valerolactone by using water-soluble and reusable iridium complexes in acidic aqueous media. *ChemSusChem* **2013**, *6*, 1163–1167.
13. Yan, Z.; Lin, L.; Liu, S. Synthesis of γ-valerolactone by hydrogenation of biomass-derived levulinic acid over Ru/C catalyst. *Energy Fuels* **2009**, *23*, 3853–3858.
14. Galletti, A.M.R.; Antonetti, C.; Luise, V.D.; Martinelli, M. A sustainable process for the production of γ-valerolactone by hydrogenation of biomass-derived levulinic acid. *Green Chem.* **2012**, *14*, 688–694.
15. Selva, M.; Gottardo, M.; Perosa, A. Upgrade of biomass-derived levulinic acid via Ru/C-catalyzed hydrogenation to γ-valerolactone in aqueous–organic–ionic liquids multiphase systems. *ACS Sustain. Chem. Eng.* **2013**, *1*, 180–189.

16. Yana, K.; Lafleura, T.; Wua, G.; Liaob, J.; Cenga, C.; Xie, X. Highly selective production of value-added γ-valerolactone frombiomass-derived levulinic acid using the robust Pd nanoparticles. *Appl. Catal. A* **2013**, *468*, 52–58.
17. Amarasekara, A.S.; Hasan, M.A. Pd/C catalyzed conversion of levulinic acid to γ-valerolactone using alcohol as a hydrogen donor under microwave conditions. *Catal. Commun.* **2015**, *60*, 5–7.
18. Ruppert, A.M.; Grams, J.; Jedrzejczyk, J.; Matras-Michalska, J.; Keller, N.; Ostojska, K.; Sautet, P. Titania-supported catalysts for levulinic acid hydrogenation: influence of support and its impact on γ-valerolactone yield. *ChemSusChem* **2015**, doi:10.1002/cssc.201403332.
19. Son, P.A.; Nishimura, S.; Ebitani, K. Production of γ-valerolactone from biomass-derived compounds using formic acid as a hydrogen source over supported metal catalysts in water solvent. *RSC Adv.* **2014**, *4*, 10525–10530.
20. Bourne, R.A.; Stevens, J.G.; Ke, J.; Poliakoff, M. Maximising opportunities in supercritical chemistry: The continuous conversion of levulinic acid to γ-valerolactone in CO_2. *Chem. Commun.* **2007**, *44*, 4632–4634.
21. Alonso, D.M.; Wettstein, S.G.; Bond, J.Q.; Root, T.W.; Dumesic, J.A. Production of biofuels from cellulose and corn stover using alkylphenol solvents. *ChemSusChem* **2011**, *4*, 1078–1081.
22. Yang, Y.; Gao, G.; Zhang, X.; Li, F. Facile fabrication of composition-tuned Ru-Ni bimetallics in ordered mesoporous carbon for levulinic acid hydrogenation. *ACS Catal.* **2014**, *4*, 1419–1425.
23. Lange, J.P.; Price, R.; Ayoub, P.M.; Louis, J.; Petrus, L.; Clarke, L.; Gosslink, H. Valeric biofuels: A platform of cellulosic transportation fuels. *Angew. Chem. Int. Ed.* **2010**, *49*, 4479–4483.
24. Braden, D.J.; Henao, C.A.; Heltzel, J.; Maravelias, C.C.; Dumesic, J.A. Production of liquid hydrocarbon fuels by catalytic conversion of biomass-derived levulinic acid. *Green Chem.* **2011**, *13*, 1755–1765.
25. Hengne, A.M.; Rode, C.V. Cu-ZrO_2 nanocomposite catalyst for selective hydrogenation of levulinic acid and its ester to γ-valerolactone. *Green Chem.* **2012**, *14*, 1064–1072.
26. Shimizu, K.; Kanno, S.; Kon, K. Hydrogenation of levulinic acid to γ-valerolactone by Ni and MoO_x co-loaded carbon catalysts. *Green Chem.* **2014**, *16*, 3899–3903.
27. Mai, E.F.; Machado, M.A.; Davies, T.E.; Lopez-Sanchez, J.A.; Teixeira da Silva, V. Molybdenum carbide nanoparticles within carbon nanotubes as superior catalysts for γ-valerolactone production via levulinic acid hydrogenation. *Green Chem.* **2014**, *16*, 4092–4097.
28. Song, J.; Wu, L.; Zhou, B.; Zhou, H.; Fan, H.; Yang, Y.; Meng, Q.; Han, B. A new porous Zr-containing catalyst with a phenate group: An efficient catalyst for the catalytic transfer hydrogenation of ethyl levulinate to γ-valerolactone. *Green Chem.* **2015**, doi:10.1039/c4gc02104e.
29. Wang, J.; Jaenicke, S.; Chuah, G.K. Zirconium-Beta zeolite as a robust catalyst for the transformation of levulinic acid to γ-valerolactone via Meerwein-Ponndorf-Verley reduction. *RSC Adv.* **2014**, *4*, 13481–13489.
30. Bermudez, J.M.; Menéndez, J.A.; Romero, A.A.; Serrano, E.; Garcia-Martinez, J.; Luque, R. Continuous flow nanocatalysis: Reaction pathways in the conversion of levulinic acid to valuable chemicals. *Green Chem.* **2013**, *15*, 2786–2792.
31. Deng, L.; Li, J.; Lai, D.; Fu, Y.; Guo, Q. Catalytic conversion of biomass-derived carbohydrates into γ-valerolactone without using an external H_2 supply. *Angew. Chem. Int. Ed.* **2009**, *48*, 6529–6532.

32. Deng, L.; Zhao, Y.; Li, J.; Fu, Y.; Liao, B.; Guo, Q.X. Conversion of levulinic acid and formic acid into γ-valerolactone over heterogeneous catalysts. *ChemSusChem* **2010**, *3*, 1172–1175.
33. Yepez, A.; Lam, F.L.Y.; Romero, A.A.; Kappe, C.O.; Luque, R. Continuous flow preparation of iron oxide nanoparticles supported on porous silicates. *ChemCatChem* **2015**, *7*, 276–282.
34. Toledano, A.; Serrano, L.; Pineda, A.; Balu, A.M.; Luque, R.; Labidi, J. Fractionation of organosolv lignin from olive tree clippings and its valorization to simple phenolic compounds. *ChemSusChem* **2013**, *6*, 529–536.
35. Toledano, A.; Serrano, L.; Labidi, J.; Balu, A.M.; Pineda, A.; Luque, R. Heterogeneously catalysed mild hydrogenolytic depolymerisation of lignin under microwave irradiation with hydrogen-donating solvents. *ChemCatChem* **2013**, *5*, 977–985.
36. Al-Shaal, M.G.; Hausoul, P.J.C.; Palkovits, R. Efficient, solvent-free hydrogenation of α-angelica lactone catalysed by Ru/C at atmospheric pressure and room temperature. *Chem. Commun.* **2014**, *50*, 10206–10209.
37. Palkovits, R. Pentenoic acid pathways for cellulosic biofuels. *Angew. Chem. Int. Ed.* **2010**, *49*, 4336–4338.